ISSN: 2447-3359

REVISTA DE GEOCIÊNCIAS DO NORDESTE

Northeast Geosciences Journal

v. 11, nº 1 (2025)

https://doi.org/10.21680/2447-3359.2025v11n1ID36612

Geospatial Assessment of the Spatio-Temporal Dynamics of the São José da Coroa Grande Coastline, Pernambuco state, Brazil

Avaliação Geoespacial da Dinâmica Espaço-Temporal da Linha de Costa de São José da Coroa Grande, Pernambuco, Brasil

Artur Loiola Alves da Silva[1]; Admilson da Penha Pacheco[2]; Eduardo Paes Barreto[3]; Maria das Neves Gregório[4]; Marcia Cristina de Souza Matos Carneiro[5]

[1] UFPE, Departamento de Engenharia Cartográfica, Recife/PE, Brasil. Email: artur.loiola@ufpe.br
ORCID: https://orcid.org/0009-0005-8308-6667

[2] UFPE, Departamento de Engenharia Cartográfica, Recife/PE, Brasil. Email: admilson.pacheco@ufpe.br
ORCID: https://orcid.org/0000-0002-3635-827X

[3] ITEP, Pós-graduação do Instituto de Tecnologia de Pernambuco, Recife/PE, Brasil. Email: eduardo.barreto@ufpe.br
ORCID: https://orcid.org/0000-0001-8301-4878

[4] UFPE, PPGCGTG, Recife/PE, Brasil. Email: nevesgregorio@hotmail.com
ORCID: https://orcid.org/0000-0003-2981-6719

[5] IBGE, Instituto Brasileiro de Geografia e Estatística, Recife/PE, Brasil. Email: carmarciaibge@gmail.com
ORCID: https://orcid.org/0000-0001-5397-6646

Abstract: Coastline monitoring is essential to understand the impact of human activities and climate change on the coastal zone. Regular monitoring of the position of the coastline is extremely important to analyze and to select the most effective engineering solutions in order to contain the coastal erosion as well as to support a sustainable coastal management system. This study aims to evaluate the evolution of the coastline in São José da Coroa Grande, Pernambuco state, over the last 49 years, using remote sensing techniques such as satellite images, unmanned aerial vehicles (UAVs), in addition to GNSS surveys. The coastal progradation and retrogradation rates were calculated, identifying the geomorphological elements that influence the changes such as erosion and sediment accumulation. The results revealed consistent patterns of erosion and accretion over the decades examined (1974, 1981, 1997 and 2023), highlighting a section with erosion of up to -114.291 m/year between 1974 and 1997. The study also highlighted seasonal dynamics of progradation and retrogradation in the area. It is recommended to integrate high spatial resolution remote sensing data and GNSS with oceanographic information for a more complete understanding of the coastal changes in future research.

Keywords: Coastline; Geospatial Technologies; Erosion.

Resumo: O monitoramento da linha de costa é essencial para compreender o impacto das atividades humanas e das mudanças climáticas na zona costeira. O acompanhamento regular da posição da linha de costa é extremamente importante para analisar e selecionar as soluções de engenharia mais eficazes na contenção da erosão costeira, além de subsidiar um sistema de gestão litorânea sustentável. Este estudo visa avaliar a evolução da linha de costa em São José da Coroa Grande, Pernambuco, ao longo dos últimos de 49 anos, usando técnicas de sensoriamento remoto como imagens de satélite, veículos aéreos não tripulados (VANT), além de levantamentos GNSS. Foram calculadas as taxas de progradação e retrogradação da costa, identificando os elementos geomorfológicos, que influenciam as mudanças, como erosão e acúmulo de sedimentos. Os resultados revelaram padrões consistentes de erosão e acreção ao longo das décadas examinadas ((1974, 1981, 1997 e 2023)., destacando um trecho com erosão de até -114,291 m/ano entre 1974 e 1997. O estudo também evidenciou a dinâmica sazonal de progradação e retrogradação na área. Recomenda-se integrar dados de sensoriamento remoto de alta resolução espacial e GNSS com informações oceanográficas para uma compreensão mais completa das mudanças costeiras em futuras pesquisas.

Palavras-chave: Linha de costa; Tecnologias Geoespaciais; Erosão.

Recebido: 11/06/2024; Aceito: 09/01/2025; Publicado: 06/02/2025.

1. Introduction

The coastline is defined as the interface between the land and the sea that is continuously subject to one or more factors, such as climatic, hydrodynamic, geological, geomorphological and human influences (ZOYSA et. al., 2023).

Climate change and its impacts, combined with uncontrolled human activities, intensify pressures on coastal environments, resulting in the modification of the coastal morphodynamics (Chowdhury et al., 2023). Thus, measuring and monitoring changes in the coast is a task for the coastal zone management, being a matter of environmental security, which is related to changes in the sea level and the evolution of the coastal zone (HUANG et al., 2020).

Currently, monitoring of coastal dynamics is carried out mainly through remote sensing techniques, such as: remote sensing from satellite images and unmanned aerial vehicles (UAVs), supported by measurements carried out through the Global Navigation Satellite System (GNSS) (HUANG et al., 2020).

The increased availability of multispectral satellite and UAV images, combined with the development of advanced digital image processing algorithms, has favored several advanced applications in coastal areas in the recent years (CAVALLI, 2024; TSIAKOS; CHALKIAS, 2024).

Many studies have proven the effectiveness of unmanned aerial vehicles (UAVs) for coastal applications (TURNER et al., 2016; VECCHI et al., 2021). The main advantages of UAVs are their low acquisition and use costs (compared to other tools), the possibility of rapid planning and the preparation of flights in the field with the help of control points acquired by GPS/GNSS. The fact that most UAVs transmit images in real time allows the experiment to be repeated in case of failure or error, in addition to the low safety risks in case of accidents (GONÇALVES; HENRIQUES, 2015).

GNSS surveys are particularly suitable for monitoring coastal areas due to the absence of obstacles that could reduce sky visibility (VECCHI et al. 2021). The most widespread approaches used in GNSS coastal surveys are those that allow real-time results: Real-Time Kinematic (RTK) and Network-RTK (NRTK) (COHEN; HÉQUETTE, 2020; GONÇALVES et al., 2017). Real-time work allows the quality of the survey to be assessed in the field by checking the state of ambiguity resolution.

Several studies on the morphological dynamics of coastal regions have been carried out in the recent decades on the coast of the state of Pernambuco (GREGÓRIO et al., 2017; GONÇALVES et al., 2019).

The municipality of São José da Coroa Grande, in Pernambuco state, has a vast coastal extension, of approximately 10 kilometers. This coastal characteristic gives it an economic vocation related to tourism and fishing activities, which leads to rapid growth in the real estate sector. Due to these aspects, the choice of the study area on São José da Coroa Grande beach was motivated by the constant erosion observed in the region, which can impact the aforementioned activities.

In this context, the objective of this study was to evaluate the spatiotemporal evolution of the coastline in São José da Coroa Grande/PE, over the last 49 years from images obtained by UAVs and satellites, with the support of field surveys with the GNSS system. The study involved calculating the variation in the rate of progradation and retrogradation on the coastline, thus allowing the identification of geomorphological elements that influence coastal dynamics, such as erosion and sediment accumulation.

2. Methodology

2.1 Study area

São José da Coroa Grande beach (Figure 1) is located 123 km from the capital Recife, in the south ‘Zona da Mata’ region of Pernambuco state, on the border with the state of Alagoas. It is positioned in the 25S time zone between the coordinates 263312.485 and 264787.911 E and 9013753.935 and 9017937.713 N. The study area is limited to the north by the Una River, where a headland is formed, and to the south by the Persinunga River, with approximately 10 km of coastline.

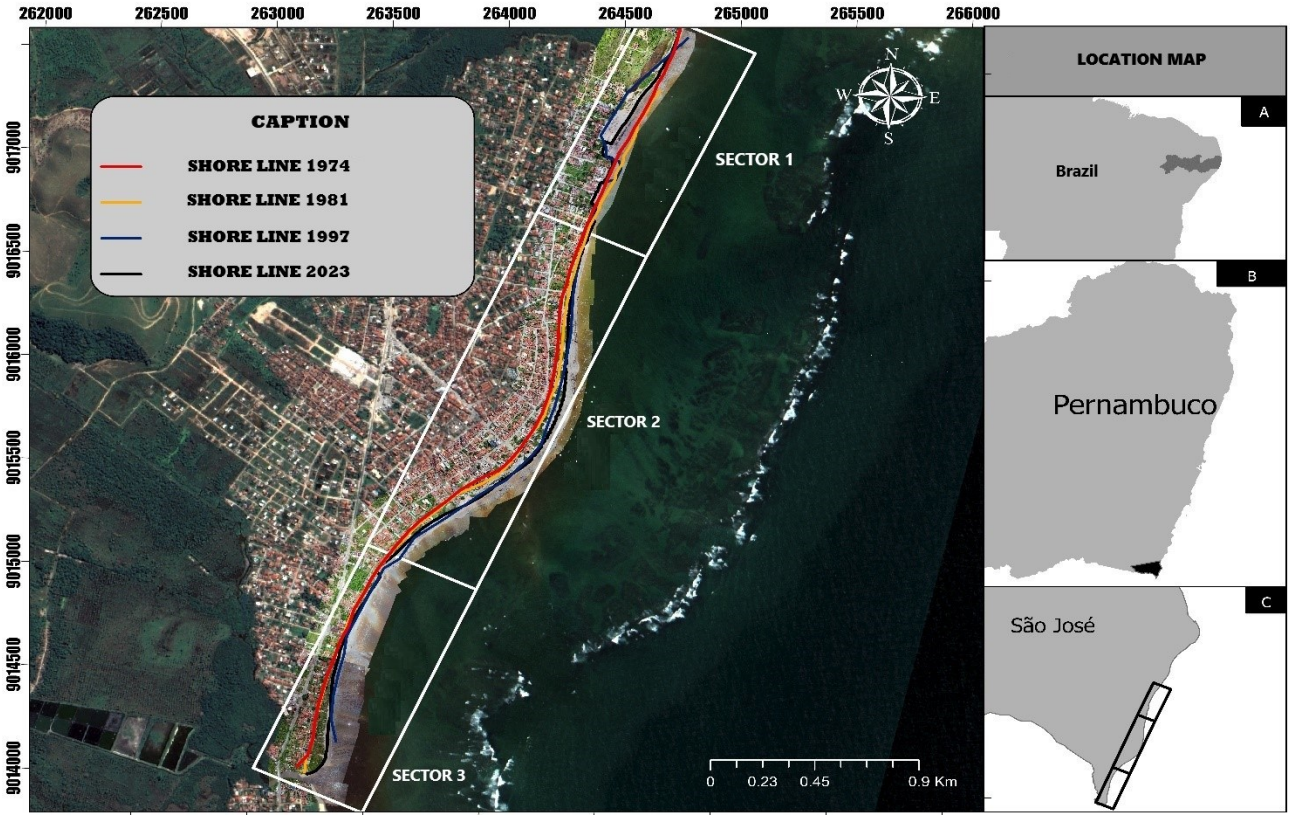

Figure 1 – Location map of the study area: **A** *- State of Pernambuco.* **B** *- Highlighting the southern coast.* **C** *- Limits by the mouths of the Una River, where a headland is formed, and the Persinunga River, with approximately 10 km of coastline.*
Source: Authors (2024).

2.2 Methodological procedures

The study involved field activities followed by subsequent data processing in a laboratory environment. The study area was subdivided into three sectors, where the field operations included the delimitation of the study area and the extraction of control points through GNSS. Figure 2 illustrates the methodological procedures adopted in this research.

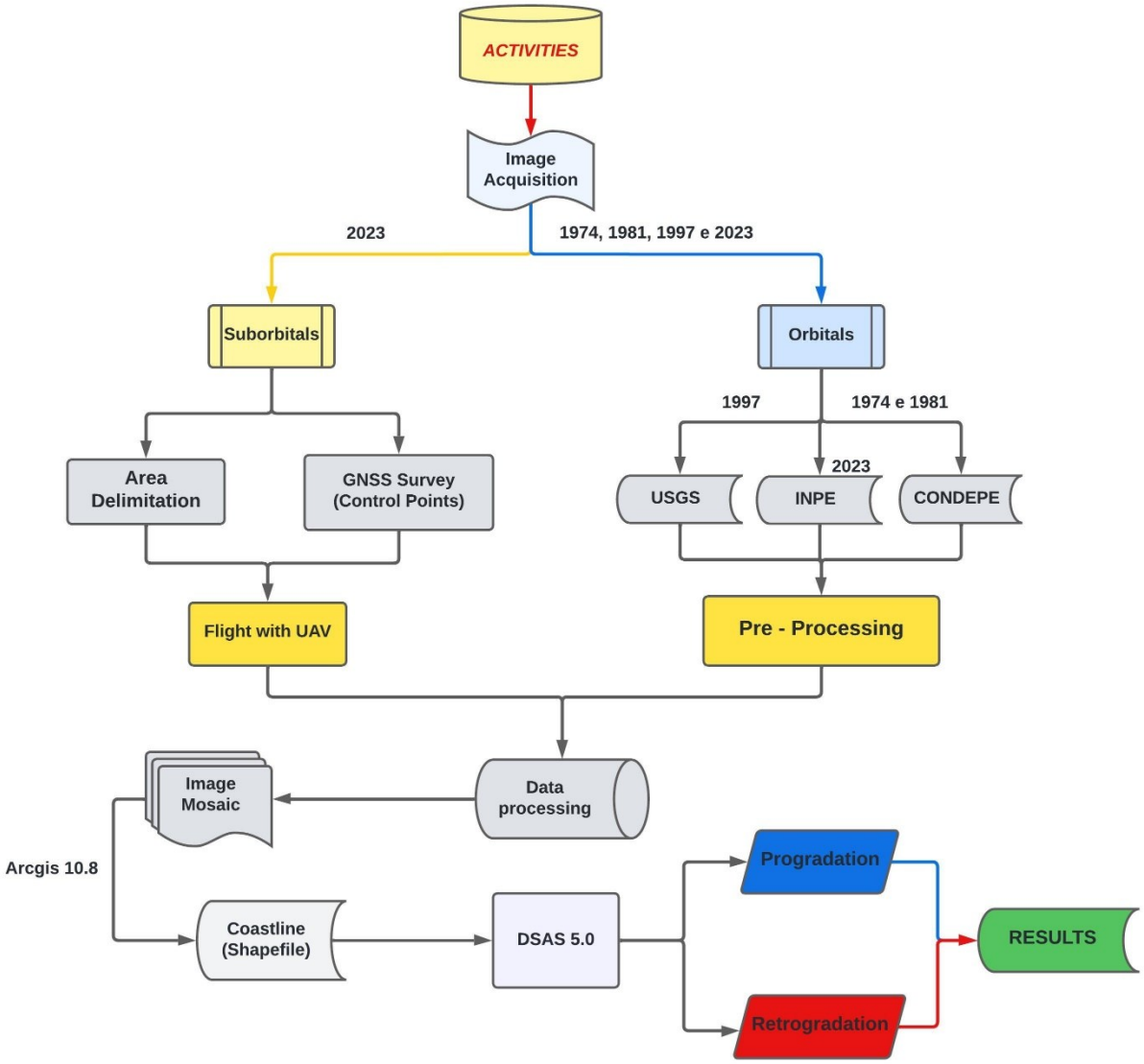

Figure 2 – Methodology Flowchart.
Source: Authors (2024).

2.2.1 Survey and processing of images with Unmanned Aerial Vehicle (UAV)

To acquire the images with an Unmanned Aerial Vehicle (UAV), it was necessary to delimit the study area using *Google Earth Pro* software. Flight plans were generated in this software. The flights covered sector 1 and part of sector 2. The DJI Phantom 4 ADVANCED UAV was used for this imaging (Table 1). The aerial photogrammetric surveys were carried out on May 6 and 7, 2023.

Table 1 – DJI Phanton 4 Advanced camera parameters.

Camera Parameters	
Sensor	CMOS 20 MP
Resolution (px)	4096×2160

Focal length (mm)	8.8
Flight height (m)	110
GSD (cm)	2.44

Source: DJI – Phantom 4 Advanced manual (2024).

The corresponding flight areas were exported in KML format and later imported into the DroneDeploy - Mapping for DJI *software*, version 4.135.0. The following flight parameters were configured using this software: I. Frontal overlap of 80%; II. Lateral overlap of 80%; III. Flight direction 152°; IV. Flight speed 2 m/s; V. Gimbal angle 90°; VI. Flight height: 110 m. The specifications mentioned above in Table 1 resulted in a total flight time of approximately 3 hours, covering an area of 81 hectares. During this period, 1840 images were captured, which required the consumption of 18 batteries.

After the flight, all images were imported into the software PIX4D mapper 4.5.4. They were then merged, calibrated and georeferenced, resulting in the final orthoimage of the study area.

2.2.2 Acquisition and processing of the control points.

The equipment Leica GS15 was used to obtain the control points. To correct first-order effects for dual-frequency receivers, the ionosphere-free linear combination can be used, which linearly combines the observable L1 and L2 frequencies (MONICO, 2008).

Equations 1 and 2 present the ionosphere-free linear combinations for the carrier wave phase φ_{IF} and the pseudorange PD_{IF}:

$$PD_{IF} = m_1 PD_{L1} + m_{2PD} PD_{L2} \quad (1)$$

$$\varphi_{IF} = m_1 \varphi_{L1} + m_{2\varphi} \varphi_{L2} \quad (2)$$

Where, m_1 and m_2 are the multiplying coefficients of the combination.

The coordinates of the points were collected using the fast static relative method (Figure 3), with a storage interval of 5 min. The data from the survey were processed using the Leica Geo Office software. The method used is based on the relative positioning technique in relation to the SAT 93110 station, which represents one of the vertices of the Brazilian Continuous Monitoring Network (RBMC).

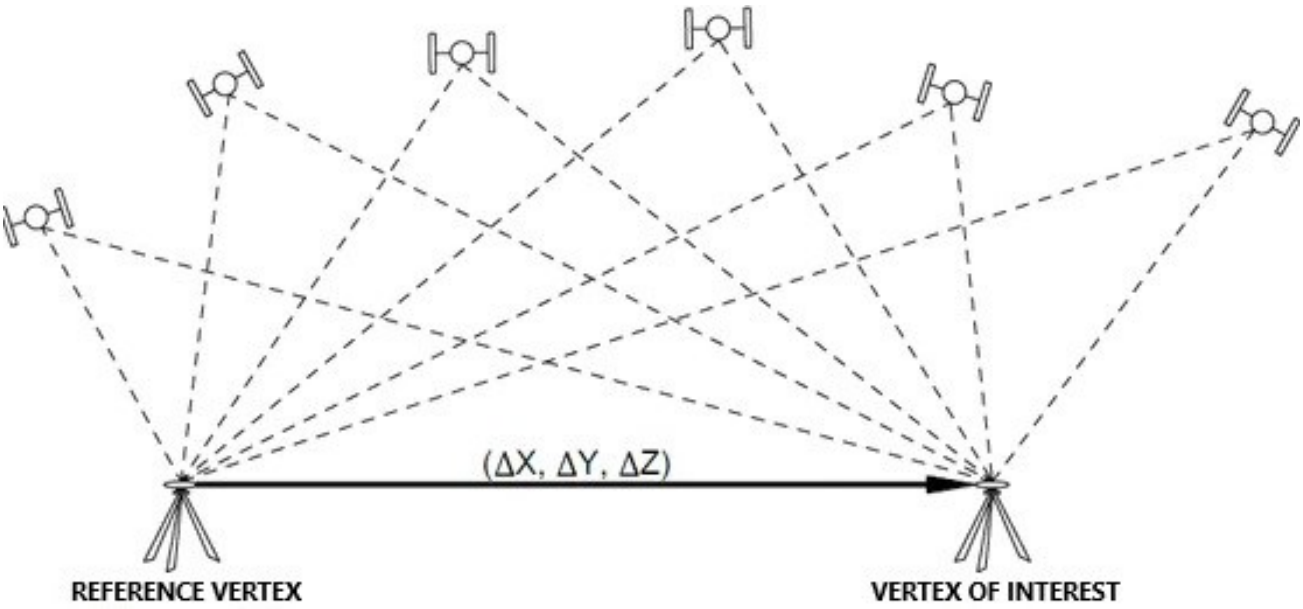

Figure 3 – Static relative method
Source: Monico (2008).

2.2.3 Acquisition and processing of orthophotos and orbital images.

The selection of images was based on the temporal aspect defined in the study, that is, the last 49 years. The orthophotos, with a spatial resolution of 04 meters, from the years 1974 and 1981, were obtained from CONDEPE/FIDEM (CONDEPE/FIDEM, 2023). The Landsat images from 1997, with a spatial resolution of 30 m, were acquired through the United States Geological Survey (USGS) website (USGS, 2023). The CBERS-4A/VPM images, with a spatial resolution of 2 m, were obtained from the image catalog of the National Institute for Space Research (INPE), (INPE, 2023). All images were georeferenced using ArcGis 10.8 software in the UTM (Universal Transversal Mercator) system and Datum – SIRGAS 2000 25S (Geocentric Reference System for the Americas).

Table 2 presents the specifications of the orthophotomaps and satellite images used in the study.

Table 2 – Specifications of orthophotomaps and satellite images.

Acquisition	Satellite	Date	Spectral bands (µm)				Resolution (m)
			B	G	R	NIR	
Condepe/Fiden (Orthophotomap)	-	01/01/1974	**0 - 0.25**	**0.04 - 0.19**	**0.04 - 0.19**	-	0.4
Condepe/Fiden (Orthophotomap)	-	01/01/1981	**0 - 0.25**	**0.04 - 0.19**	**0.04 - 0.19**	-	0.4
USGS	LANDSAT-5 TM	04/10/1997	**0.45 - 0.52**	**0.50 - 0.60**	**0.63 - 0.69**	-	30
INPE	CBERS-4A WPM	07/05/2023	**0.45 - 0.52**	**0.52 - 0.59**	**0.63 - 0.69**	**0.77 - 0.89**	2

Source: Authors (2024).

The images from 1997 and 2023 were processed with the Qgis 3.34.3 software. The RGB spectral bands were mosaicked using the raster > miscellaneous > mosaic tools. The 2023 image from the CBERS4A satellite needed to undergo a pansharpening process, which consists of transforming the multispectral image into a suitable domain, where one of the components is replaced by the high spatial resolution panchromatic image (PAN).

2.2.4 Coastline Extractions

The high tide shoreline was used to vectorize the images. The coastline variation rates were determined using the end point rate (EPR) and linear regression rate (LRR) methods using the tool DSAS 5.0, acquired from the USGS, and later installed as an extension in the Argcis 10.8 software. These rates, expressed in meters per year (m/year), can be negative, positive or zero, indicating retreat, advance or stability of the coastline, respectively (GALGANO; DOUGLAS, 2000). From this process, a line-type shapefile was generated from which it was possible to extract the coastline from the images. These data were then imported into DSAS (Digital Shoreline Analysis System), where a geodatabase was created and a straight line parallel to the coastline was established. Using these data, the software processed all relevant statistical information associated with the coastal analysis.

3. Results and discussion

The delimitation of the coastline of the beaches of the municipality of São José da Coroa made it possible to assess the space-time over the last 49 years through remote sensing and the classification of erosion, accretion and equilibrium processes (Figure 4). It was thus possible to identify changes and/or trends in the dynamics of the coastline.

Figure 4 presents the map of temporal variation of the coastline in the periods 1974 to 1981, 1974 to 1997 and 1974 to 2023, qualitatively characterizing the erosion and accretion processes. A detailed approach is presented by sectors (1, 2 and 3) below.

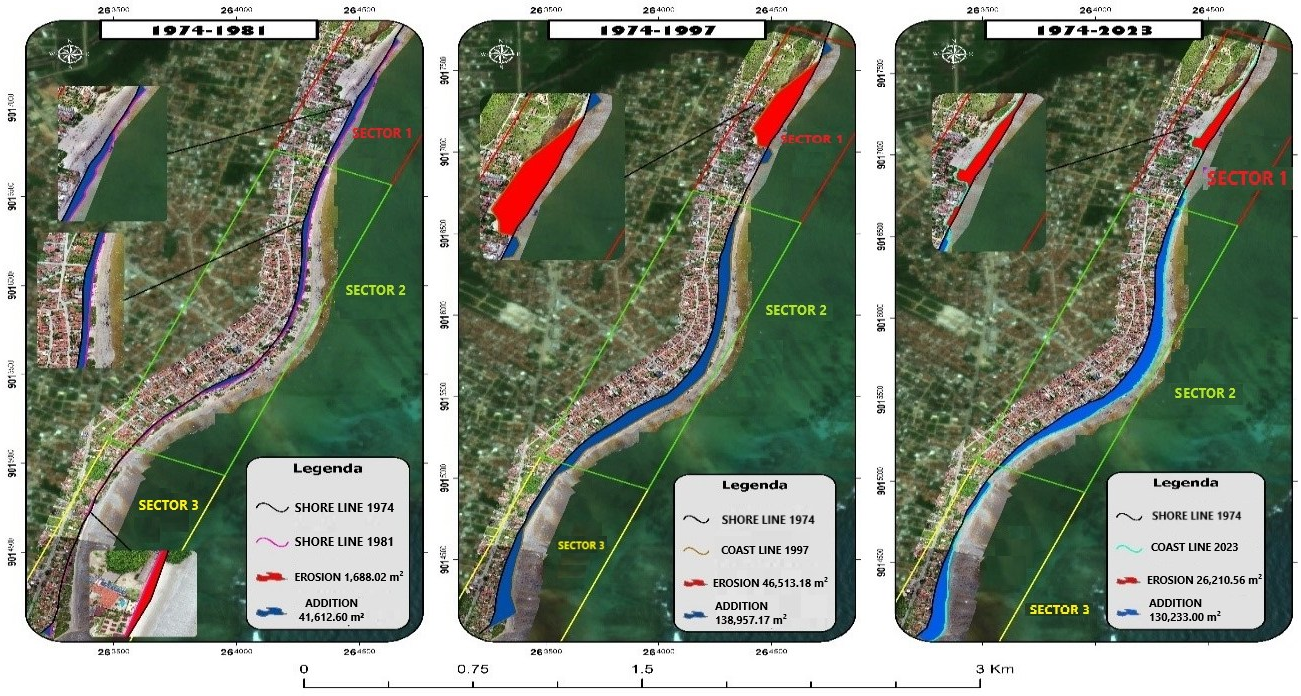

Figura 4 – Mapa da variação temporal da linha de costa.
Fonte: Authors (2024).

a) Sector 1

Between 1974 and 1981, sector 1, located in the northernmost part of the study area, experienced progradation of the coastline, with an average positive rate of 2.54 m/year (Table 2, Figure 4). During this period, the greatest minimum variation was also recorded, reaching 0.59 m/year (Table 2), accompanied by a standard deviation of 1.04 m/year. From 1974 to 1997, a retrogradation movement of the coastline was observed, with the highest average negative rate of -1.40 m/year (Table 2, Figure 5). Furthermore, this period recorded the lowest minimum value of variation rates, reaching -4,11 m/year (Table 2), accompanied by the highest standard deviation, reaching 1.91 m/year, the highest among the years.

Between 1974 and 2023, a retrogradation of the coastline was observed, but with an average negative rate of -0.42 m/year (Table 2, Figure 4). This period recorded the minimum value of -1.49 m/year (Table 2), with a standard deviation between sectors of 0.45 m/year, the lowest among the years.

Table 2 – Variations in rates (m/year) of coastline displacement in sector 1.

SECTOR 1	Number of Transects	Mean	Minimum	Maximum	Standard deviation
1974 – 1981	377	2.54	0.59	4.40	1.04
1974 – 1997	518	-1.40	-4.11	1.57	1.91
1974 – 2023	529	-0.42	-1.49	0.45	0.45

Source: Authors (2024).

Regarding the average values of the variation in coastline displacement distances from 1974 to 1981, there was the highest positive average among all sectors, recording a value of +17.79 m (Table 3) in a segment of approximately 752 m in length, indicating progradation of the coastline (Figure 5). In addition, the minimum and maximum values of the distances were respectively +4.18 m and +30.83 m, while the standard deviation was the lowest found, at 7.28 for the period studied.

In the interval from 1974 to 1997, in relation to the average values of the variation in coastline displacement distances, sector 1 exhibited the lowest average among all sectors, recording a value of -39.01 m/year (Table 3) in a segment of approximately 1034 m in length, indicating retrogradation of the coastline (Figures 4 and 5). Furthermore, the minimum and maximum distance values were -114.29 m/year and +43.84 m/year, respectively, while the standard deviation was the highest, 53.02 m/year for the period studied.

As for the period from 1974 to 2023, an average of -22.66 m/year was recorded (Table 3) in a segment of approximately 1057 m in length, confirming a retrogradation in the coastline (Figures 4 and 5). Likewise, the minimum and maximum distance values were -79.58 m/year and +24.53 m/year, respectively, while the standard deviation was 24.53 m/year for the period studied.

Table 3 – Variations in distances in the displacement of the coastline sector 1.

DISTANCES (m)

SECTOR 1	Number of Transects	Mean	Minimum	Maximum	Standard deviation
1974 – 1981	377	17.79	4.18	30.83	7.28
1974 – 1997	518	-39.01	-114.29	43.84	53.02
1974 – 2023	529	-22.66	-79.58	24.53	24.53

Source: Authors (2024).

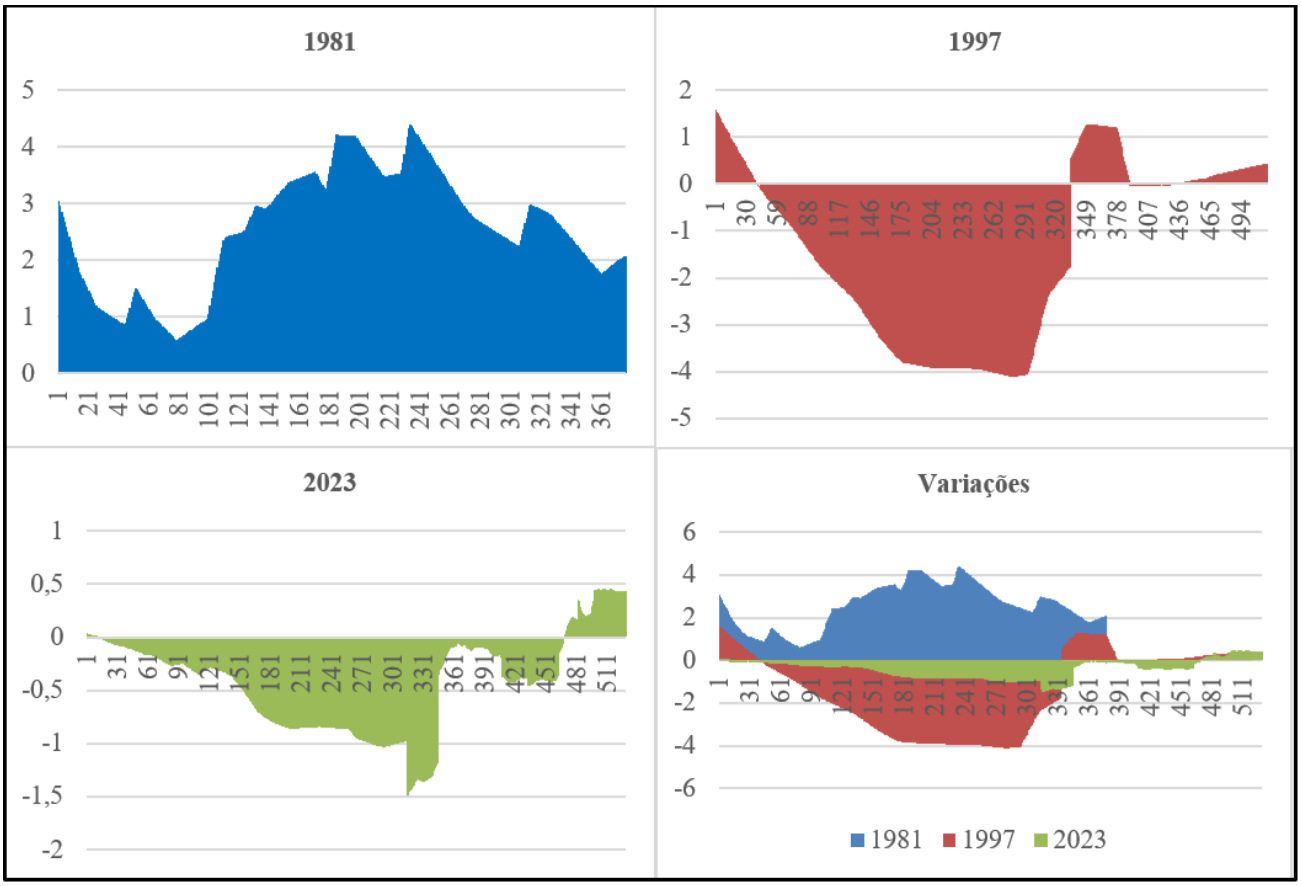

Figure 5 – Variation in progradation and retrogradation rates in sector 1.
Source: Authors (2024).

b) Sector 2

During the period from 1974 to 1981, sector 2 stood out as the most relevant among the examined sectors, recording a positive average of 2.10 m/year for the coastline variation (Table 4, Figure 5). In addition, the sector presented the maximum value of the rate, reaching +4.22 m/year, which represented the highest value observed throughout the years considered. At the same time, the sector also exhibited the largest standard deviation, reaching 1.07 m/year. Thus, presenting a progression for the period from 1974 to 1981 (7 years). Between 1974 and 1997, sector 2 demonstrated the second highest positive average among the periods analyzed, with an average coastline variation rate of 1.80 m/year (Table 3, Figure 5). In addition, the maximum value recorded for the rate was +2.82 m/year, still representing a significant rate.

Additionally, the standard deviation obtained was the second lowest, totaling 0.58 m/year, thus showing a progradation for the period from 1974 to 1997 (23 years).

For the interval from 1974 to 2023, sector 2 revealed the lowest positive average among the periods analyzed, with an average coastline variation rate of 0.95 m/year (Table 3, Figure 5). The maximum value recorded was +1.63 m/year, the lowest among the sectors considered. In addition, it presented the lowest standard deviation, totaling 0.34 m/year, thus showing a progradation for the period from 1974 to 2023 (49 years).

Table 4 – Variations in rates (m/year) of coastline displacement in sector 2.

SECTOR 2	Number of Transects	Mean	Minimum	Maximum	Standard deviation
1974 – 1981	884	2.10	0.26	4.22	1.07
1974 – 1997	885	1.80	0.44	2.82	0.58
1974 – 2023	885	0.95	0.29	1.63	0.34

Source: Authors (2024).

Regarding the average values of variation in coastline displacement distances in sector 2, during the period from 1974 to 1981, the average was 14.71 m/7 years (Table 5, Figure 6), with a minimum of 1.82 m/7 years and the lowest standard deviation recorded was 7.49 m/year.

Between 1974 and 1997, the average value of variation in distances in sector 2 was 50.11 m/23 years (Table 5, Figure 6), the second highest recorded over the years. The minimum recorded was 12.26 m/23 years (Table 5), with a standard deviation of 16.27 m/year.

For the period from 1974 to 2023, the average variation in distances in sector 2 was 50.83 /49 years (Table 5, Figure 6), the highest among all sectors. The minimum recorded was 15.70 m/49 years, with the largest standard deviation recorded, of 18.49 meters (Table 5).

Table 5 – Variations in distances in the displacement of the coastline sector 2.

DISTANCES (m)

SECTOR 2	Number of Transects	Mean	Minimum	Maximum	Standard deviation
1974 – 1981	884	14.71	1.82	29.54	7.49
1974 – 1997	885	50.11	12.26	78.46	16.27
1974 – 2023	885	50.83	15.70	87.36	18.49

Source: Authors (2024).

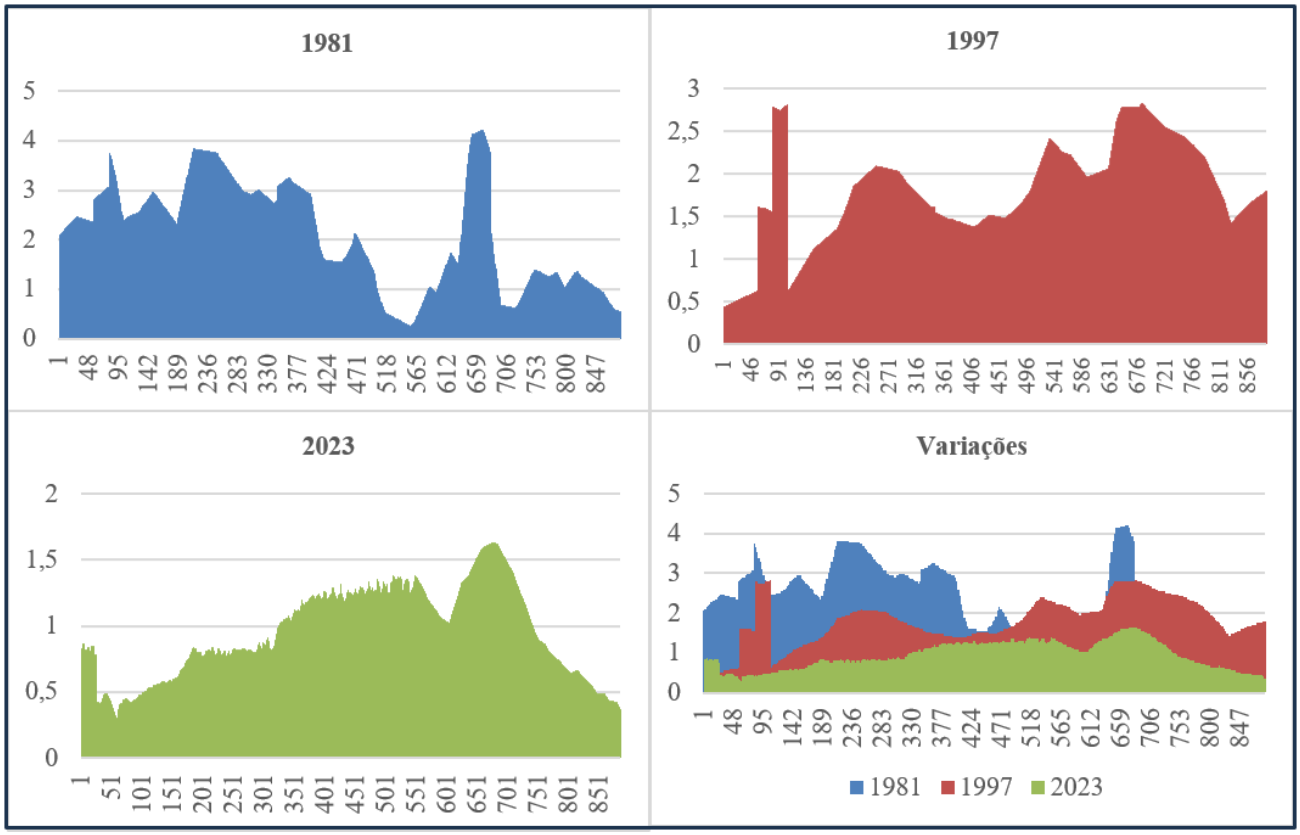

Figure 6 – Variation in progradation and retrogradation rates in sector 2.
Source: Authors (2024).

c) Sector 3

During the period 1974 to 1981, the average coastline displacement rate in sector 3, located to the south of the study area, was 0.18 m/year, indicating an advancing movement (Table 6, Figure 7). The highest value recorded was 5.44 m/year, while the lowest was -1.07 m/year, with a standard deviation of 0.81.

Between 1974 and 1997, the average coastline displacement rate was 1.40 m/year, also showing an advancing movement (Table 6, Figure 7). The second highest rate recorded was 3.78 m/year, with a minimum of 0.46 m/year and a standard deviation of 0.78 m.

In the interval from 1974 to 2023, the average rate was 0.63 m/year (Table 6, Figure 7), indicating a progradation movement (Figures 3 and 6). The maximum observed rate was 1.48 m/year, while the minimum was 0.008 m/year, with a standard deviation of 0.46, the lowest among the years analyzed.

Table 6 – Variations in rates (m/year) of coastline displacement in sector 3.

SECTOR 3	Number of Transects	Mean	Minimum	Maximum	Standard deviation
1974 – 1981	551	0.18	-1.07	5.44	0.81
1974 – 1997	461	1.40	0.46	3.78	0.78
1974 – 2023	550	0.63	0008	1.48	0.46

Source: Authors (2024).

In sector 3, during the period from 1974 to 1981, an average variation in distances (Table 7 and Figure 7) of 1.27 m/7 years was observed, representing the lowest average between the years and therefore indicating an advance in the coastline for this sector (Figures 6). This period also recorded the lowest maximum rate of 38.09 m/7 years and the lowest minimum rate of -7.55 m/7 years, with a standard deviation of 5.73 m/7 years, the lowest among all the years analyzed (Table 7, Figures 3 and 6).

Between 1974 and 1997, an average variation in distances (Table 6 and Figure 6) of 38.94 m/23 years was observed, indicating an advance in the coastline for this sector (Figures 5 and 6). During this period, the highest maximum rate recorded was 105.09 m/23 years, with a minimum rate of 12.99 m/23 years and a standard deviation of 21.66 m/year (Table 7).

Over the period from 1974 to 2023, an average variation in distances (Table 7; Figures 4 and 7) of 34.15 m/49 years was observed, indicating an advance in the coastline for this sector (Figures 4 and 7). This period presented a maximum rate of 79.68 m/49 years and a minimum rate of 0.44 m/49 years, with a standard deviation of 24.96 m/year (Table 7), the highest among the years analyzed.

Table 7 – Variations in distances in the displacement of the coastline sector 3.

	DISTANCES (m)				
SECTOR 3	Number of Transects	Mean	Minimum	Maximum	Standard deviation
1974 – 1981	551	1.27	-7.55	38.09	5.73
1974 – 1997	461	38.94	12.99	105.09	21.66
1974 – 2023	550	34.15	0.44	79.68	24.96

Source: Authors (2024).

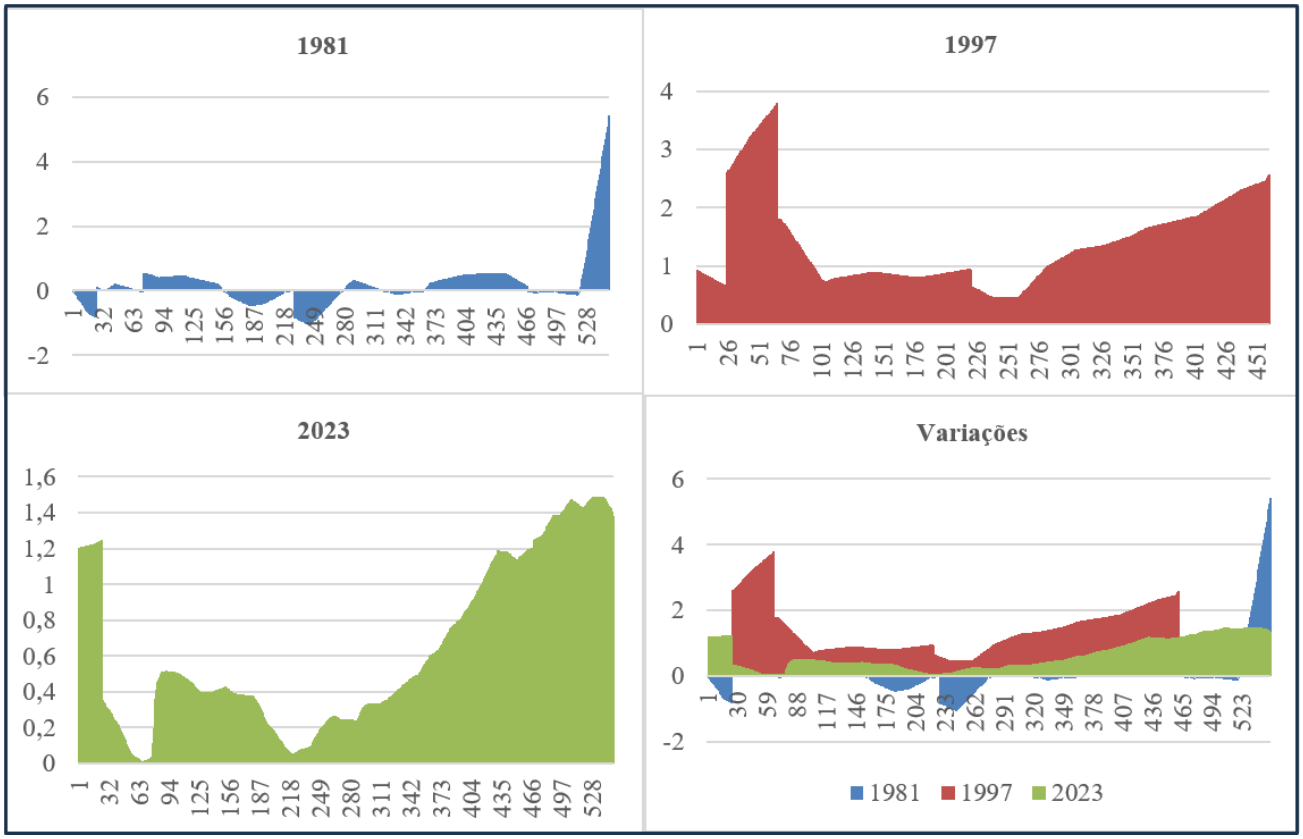

Figure 7 – Variation in progradation and retrogradation rates in sector 3.
Source: Authors (2024).

d) Transgression and Regression in Sectors (1, 2 and 3).

The results regarding transgression and regression in the area of the 3 sectors between 1974 and 1981 (Figure 4) revealed a total retrogradation of approximately 1688.02 m² (3.9%), while the progradation areas on the coast totaled 41,612.60 m² (96.1%).

The variation in the coastline demonstrated an addition of approximately 13,720.09 m² of progradation area in sector 1 during the 7-year period (1974-1981). In sector 2, this variation was even more significant, reaching 25,983.07 m² of progradation area, highlighting it as the sector with the greatest accretion. Meanwhile, in sector 3, the variation was 249.1 m² over the same period (Figure 4).

The results obtained for the area in relation to transgression and regression (Figure 4) showed a total for retrogradation of approximately 46,486.6 m² (25%), while 138,957.1 m² (75%) of progradation.

The variation of the coastline showed erosion in sector 1, approximately -39,680.13 m² of retrogradation area in a period of 23 years (1974-1997), being the only sector where transgression occurred. In sector 2, the variation was 89,007.05 m² of progradation area, showing that it is the sector with the greatest accretion. While the variation in sector 3 was 43,224.20 m² in the period of 23 years (Figure 4). The results of the analysis of the area in relation to transgression and regression (Figure 4) over the period from 1974 to 2023 revealed a total retrogradation of approximately 26,210.56 m² (16.75%), while 130,233 m² (83.25%) represented the progradation areas.

Erosion was observed on the coastline of sector 1, with a decrease of approximately -24,061.57 m² of retrogradation area over 49 years (1974-2023), this being the only sector where there was transgression. In sector 2, the variation was 89,975.05 m² of progradation area, showing it as the sector with the greatest accretion. Meanwhile, in sector 3, the variation was 38,143.59 m² over the same period (Figure 3).

4. Discussion

Regarding sector 1, there is a clear trend of coastal erosion. This is evidenced by the significant variation in results over the years. Between 1974 and 1981, the sector experienced a progradation process, with an average positive rate of 2.54 m/year (Table 2, Figure 5) and a minimum variation of 0.59 m/year. Subsequently, this scenario turned into retrogradation, reaching its maximum point between 1974 and 1997, with average negative rates of -1.40 m/year (Table 1, Figure 4). This period is also characterized by the lowest variation rates, reaching up to -4.11 m/year. In the period from 1974 to 2023, the negative erosion averages decreased, with an average of -0.42 m/year and minimum values of -1.49 m/year (Table 1), indicating a sector subject to an intense transgression process (Figures 4 and 5). The dynamics of the coastline of sector 1 are similar to what was found by FOTSI et al. (2019), who examined the Wouri estuary, located in the Gulf of Guinea. In this study, the period from 1948 to 1996 was covered, revealing that 35% or 29.13 km² of the investigated area demonstrated erosion in zone 1 of the study site. In addition to them, other authors obtained similar results, as we can see in the study carried out by SILVA et. al. (2021), where Paiva beach (Cabo de Santo Agostinho, PE state, Brazil) was analyzed, obtaining the result of 31% of the coastline transgression area.

Human activities have reduced the sediment supply to coastal areas (DAS et al., 2021; HAPKE et al., 2013), while sea level rise has impacted the sediment budget in all regions (FORBES et al., 2004). Increased erosion of coastal environments is expected, particularly due to projected sea level rise resulting from human-induced climate change (HAPKE et al., 2013).

Sector 2 demonstrated progradation of the coastline over time, as evidenced by statistical values in all analyzed periods. In the period from 1974 to 1981, average rates of 2.10 m/year were recorded, with a minimum variation of 0.26 m/year (Table 4). Between 1974 and 1997, the sector presented an average distance between transects of 50.11 m, with a minimum of 12.26 m, which positions it as the interval with the second greatest regression. The highest average and minimum distance values were observed in the time interval 1974 - 2023, with 50.83 m and 15.70 m, respectively (Table 5; Figures 4 and 6). These trends can be explained by the progressive stock of sediments in the northern portions of the beach arches due to the action of longshore drift currents (Vos et al., 2019), by the reworking of previously deposited sediments and by changes related to waves (Silva et al., 2016).

The results of this study are in line with those carried out by Barreto (2014) in the corresponding study area, where sector 2, during the period from 1960 to 2013 (53 years), presented results comparable to the current ones. In this context, the average distance between transects was 47.24 meters, while the minimum distance was 12.25 meters. This shows a continuous progradation of the coastline in this sector.

Examining sector 3 in the time interval from 1974 to 1981, we can show that even with erosion points, considering its minimum rates of -1.07 m/year and minimum distance of -7.55 m, this sector presents average rates of 0.18 m/year, thus being an area of progradation. The continuity of sediment accumulation in the study area is evidenced in the results of subsequent years, with average rates and average distances of 1.40 m/year and 38.94 m (Tables 6 and 7) respectively between 1974 and 1997. While in the time interval 1974-2023, the average rates are 0.63 m/year and the average distance is 34.15 m (Tables 6 and 7; Figures 4 and 7).

The incidente waves on the beach are a factor that determines the occurrence of erosional or sedimentation coasts (UMAR et al., 2015). Progradation is generated when the reef line is continuous, the beach advances forming a tombolo (COUTINHO, 1997). According to SANTOS JUNIOR et al. (2020), these processes are influenced by a series of additional factors, such as winds, sea currents, tidal variations and, in the specific context of Pernambuco state, events of greater rainfall that can lead to flooding in urban coastal areas, resulting in an increase in sediment transport by rivers.

5. Final Considerations

The results of this study revealed a consistent pattern of changes in erosion and accretion of the coastline over the four decades examined (1974, 1981, 1997 and 2023). Along with continuous transgression to the north of the area, representing 16.55% in sector 1, while sector 2 registered a cumulative regression of 59.69% throughout the analyzed period. Although small areas of erosion were identified in the 1980s, sector 3, to the south of the study area, presented regression rates of 23.77%.

The study highlighted the seasonal dynamics of progradation and retrogradation in all sectors throughout the periods investigated. In sector 1, for example, a continuous retreat of the coastline was observed over the years, causing significant impacts on the local community. Previous studies corroborate the hypothesis that variations in the coastline are cyclical events, influenced by both natural factors and human activities.

Future studies are recommended to integrate high spatial resolution remote sensing data (obtained from satellite and UAV images) with oceanographic information, providing a more comprehensive understanding of coastline changes. In

addition, it is imperative to quantify and correlate climate variables with coastline changes, aiming at more effective management of coastal environments and mitigation of the impacts of erosion, transport and sediment deposition.

Acknowledgements

To the Pro-Rectory of Research and Innovation (Propesqi - UFPE), which financed this research through the granting of a scholarship from the Institutional Scientific Initiation Scholarship Program (PIBIC) and to businesswoman Mônica Zeneide da Silva Rodrigues, owner of Costa Dourada VILLAGE/Maragogi/Alagoas state, for logistical support for the research.

References

Armenio, E.; De Serio, F.; Mossa, M.; and Petrillo, A. F. Coastline evolution based on statistical analysis and modeling, Nat. *Hazards Earth Syst. Sci*., v. 19, 1937–1953, 2019. https://doi.org/10.5194/nhess-19-1937-2019, 2019.

Barreto, E. P. (2014). Processos Morfodinâmicos, Sedimentológicos e Geomorfológicos na Plataforma Continental Interna da Praia de São José da Coroa Grande, Litoral Sul de Pernambuco, Nordeste do Brasil. Recife, 2014. 309 f. Tese (Doutorado em Geociências). Programa de Pós-Graduação em Geociências, Universidade Federal de Pernambuco.

Barry, P.; Coakley, R. Accuracy of Uav Photogrammetry Compared with Network RTK GPS. Int. Arch. Photogramm. *Remote Sensing*, v. 2, 2731, 2013. https://doi.org/10.1016/j.aej.2021.04.011.

Camfield, F. E.; Morang, A. Defining and interpreting shoreline change. *Ocean & Coastal Management*, v. 32, n. 3, 129-151, ISSN 0964-5691, https://doi.org/10.1016/S0964-5691(96)00059-2 , 1996.

Cavalli, R.M. Remote Data for Mapping and Monitoring Coastal Phenomena and Parameters: A Systematic Review. *Remote Sensing, v. 16*, n. 446, 2024, https://doi.org/10.3390/rs16030446.

Chowdhury, P.; Lakku, N. K. G.; Susana Lincoln, S.; Jaya Kumar Seelam, J. K.; Ranjan Behera, M. R. "Climate change and coastal morphodynamics: Interactions on regional scales." *Science of The Total Environment*, v. 899, 166432, 2023. https://doi.org/10.1016/j.scitotenv.2023.166432

CONDEPE/FIDEM. Agência Estadual de Planejamento e Pesquisas de Pernambuco. Cartografia e Uso do Solo. *In Cartografia e Uso do Solo*. Disponível em: http://www.condepefidem.pe.gov.br/web/condepe-fidem/produtos. Acesso em: 08/09/2023.

Das, S.; Sangode, S. J.; Kandekar, A. M. Recent decline in streamflow and sediment discharge in the Godavari basin, India (1965–2015). *Catena*, v. 206, 105537, 2021. https://doi.org/10.1016/j.ecoser.2017.09.008

DJI. MANUAL PHANTON 4 ADVANCED. *In MANUAL PHANTON 4 ADVANCED.* Disponível em: https://www.dji.com/br/mobile/support/product/phantom-4-adv. Acesso em: 12 de abr de 2024.

Forbes, D. L.; Parkes, G. S.; Manson, G. K.; Ketch, L. A. Storms and shoreline retreat in the southern Gulf of St. Lawrence. *Marine Geology* v. 210, 169–204, 2004. https://doi.org/10.1016/j.margeo.2004.05.009

Fotsi, Y. F.; Pouvreau, N.; Brenon, I.; Onguene, R.; Etame, J. Temporal (1948–2012) and Dynamic Evolution of the Wouri Estuary Coastline within the Gulf of Guinea. *Journal of Marine Science and Engineering*, v.7, n.10, 343, 2019. https://doi.org/10.3390/jmse7100350

Galgano, F. A.; Douglas, B. C. Shoreline position prediction: method sand erros. *Environmental Geosciences*, v. 7, n. 1, p. 23-31, 2000. DOI: 10.1046/j.1526- 0984.2000.71006.x.

Gonçalves, J. A.; Henriques, R. UAV photogrammetry for topographic monitoring of coastal areas. *ISPRS Journal of Photogrammetry and Remote Sensing.* v. 104, 101–111, 2015. https://doi.org/10.1016/j.isprsjprs.2015.02.009

Gonçalves, R. M.; Awange, J. L. Three Most Widely Used GNSS-Based Shoreline Monitoring Methods to Support Integrated Coastal Zone Management Policies. *Journal of Surveying Engineering* v. 143, n. 3, 05017003, 2017. https://doi.org/10.1061/(ASCE)SU.1943-5428.0000219

Gonçalves, R. M.; Saleem, A.; Queiroz, H. A. A., & Awange, J. L. A fuzzy model integrating shoreline changes, NDVI and settlement influences for coastal zone human impact classification. *Applied Geography*, v. 113, 102093, 2019. doi:10.1016/j.apgeog.2019.102093.

Gregório, M. D. N.; Araújo, T. C. M. D.; Mendonça, F. J. B.; Gonçalves, R. M.; Mendonça, R. L. Mudanças posicionais da linha de costa nas praias do Pina e de Boa Viagem, Recife, PE, Brasil. *Tropical Oceanography*, Recife, v. 45, n. 1, p. 44-61, 2017.

Hapke, C. J.; Kratzmann, M. G.; Himmelstoss, E. A. Geomorphic and human influence on large-scale coastal change. *Geomorphology* v. 199, 160–170, 2013. https://doi.org/10.1016/j.geomorph.2012.11.025

Huang, C.; Zhang, H.; Zhao, J. High-Efficiency Determination of Coastline by Combination of Tidal Level and Coastal Zone DEM from UAV Tilt Photogrammetry. *Remote Sening,* v. 12*, 2189, 2020.* https://doi.org/10.3390/rs12142189

INPE – Instituto Nacional de Pesquisas Espaciais. disponível em http://www.dgi.inpe.br/catalogo/explore, Acesso em: 05/12/2023.

Junior, G. S. S.; Gregório, M. N.; Carneiro, M. C. S. M.; Barreto, E. P., COSTA, G. J. A.; & Melo, W. D. A. Análise da evolução da linha de costa da Região Metropolitana Sul da Cidade do Recife – PE, Brasil. *Revista Brasileira de Geografia Física*, v. 13, n.4, 1645-1674, 2020. https://doi.org/10.26848/rbgf.v13.4.p1645-1674

Kulp, S. A.; Strauss, B. H. New elevation data triple estimates of global vulnerability to sea-level rise and coastal flooding. *Nature Communications*, v. 10, 4844, 2019. https://doi.org/10.1038/s41467-019-12808-z

Martínez, M. L.; Intralawan, A.; Vázquez, G.; Pérez-Maqueo, O.; Sutton, P.; Landgrave, R. The coasts of our world: ecological, economic and social importance. *Ecological Economics*, v. 63, 254–272, 2007. https://doi.org/10.1016/j.ecolecon.2006.10.022

Monico, J. F. G. Posicionamento pelo GNSS: descrição, fundamentos e aplicações. 2. ed. São Paulo: *Editora UNESP*, 2008. 477p.

Ruži´C, I.; Marovi´C, I.; Benac, C.; Ili´C, S. Coastal cliff geometry derived from structure-from-motion photogrammetry at Stara Baška, ˇ Krk Island, Croatia. *Geo-Marine Letters*, 34, 555–565, 2014. https://doi.org/10.1007/s00367-014-0380-4

Santos Junior, G. S., Gregório, M. N., Carneiro, M. C. S. M., Barreto, E. P., COSTA, G. J. A.; Melo, W. D. A. Análise da evolução da linha de costa da Região Metropolitana Sul da Cidade do Recife – PE, Brasil. Revista Brasileira de Geografia Física, 13(4), 1645-1674, 2020.

Silva, C. F.A.; Schuler, C. A. B.; Gregório, M. N.; Barreto, E. P.; Marquetti, R. K. Evolução Multi-Temporal da Linha de Costa da Praia do Paiva, Litoral Sul de Pernambuco, Brasil. *Anuário do Instituto de Geociências*, 44, 41336, 2021. https://doi.org/10.11137/1982-3908_2021_44_41336

Silva, G. V.; Muler, M.; Prado, M. F.; Short, A. D.; Klein, A. H. F.; Toldo, E. E. Shoreline change analysis and insight into the sediment transport path along Santa Catarina Island north shore, Brazil. *Journal of Coastal Research*, v.32, n.4, 863-874, 2016. https://doi.org/10.2112/JCOASTRES-D-15-00164.1

Tsiakos, C.-A.D.; Chalkias, C. Use of Machine Learning and Remote Sensing Techniques for Shoreline Monitoring: A Review of Recent Literature. Applied. Sciences, v. 13, 3268, 2023. https://doi.org/10.3390/app13053268

Turner, I. L.; Harley, M. D.; Drummond, C. D. UAVs for Coastal Surveying. *Coastal Engineering*, v. 114, 19–24, 2016. https://doi.org/10.1016/j.coastaleng.2016.03.011

Umar, H.; Rahman, S.; Baeda, A. Y.; Klara, S.. Identification of coastal problem and prediction of coastal erosion sedimentation in South Sulawesi. Procedia Engineering v. 116, 125-133, 2015.

USGS - United States Geological Survey. Earth Explorer data. *In Earth Explorer data*. Disponível em: https://earthexplorer.usgs.gov/. Acesso em: 12/12/2023.

Vallet, J.; Panissod, F.; Strecha, C.; Tracol, M. Photogrammetric Performance of an Ultra Light Weight Swinglet "UAV". Int. Arch. Photogramm. *Remote Sens. Spat. Inf. Sci*. 2012, XXXVIII-1/C22, 253–258. https://doi.org/10.5194/isprsarchives-XXXVIII-1-C22-253-2011

Vecchi, E.; Tavasci, L.; De Nigris, N.; Gandolfi, S. GNSS and Photogrammetric UAV Derived Data for Coastal Monitoring: A Case of Study in Emilia-Romagna, Italy. *Journal of Marine Science and Engineering*, v. 9, 1194, 2021. https:// doi.org/10.3390/jmse9111194

Vos, K.; Harley, M. D.; Splinter, K. D.; Simmons, J. A.; Turner, I. L. (2019). Sub-annual to multi-decadal shoreline variability from publicly available satellite imagery. *Coastal Engineering*, v. 150, 160-174, 2019. https://doi.org/10.1016/j. coastaleng.2019.04.004

Zoysa, S.; Basnayake, V.; Samarasinghe, J. T.; Gunathilake, M. B.; Kantamaneni, K.; Muttil, N.; & Rathnayake, U. (2023). Analysis of Multi-Temporal Shoreline Changes Due to a Harbor Using Remote Sensing Data and GIS Techniques. *Sustainability*, v. *15*, n. 9, 7651. https://doi.org/10.3390/su15097651